Crop area and leaf area index simultaneous retrieval based on spatial scaling transformation

FAN WenJie[*], YAN BinYan & XU XiRu

Institute of RS and GIS, Peking University, Beijing 100871, China

Accurate estimation of crop yields is crucial for ensuring food security. However, crops are distributed so fragmentally in China that mixed pixels account for a large proportion in moderate and coarse resolution remote sensing images. As a result, unmixing of mixed pixel becomes a major problem to estimate crop yield by means of remote sensing method. Aimed at mixed pixels, we developed a new method to introduce additional information contained in the spatial scaling transformation equation to the canopy reflectance model. The crop area and *LAI* can be retrieved simultaneously. On the basis of a precise and simple canopy reflectance model, directional second derivative method was chosen to retrieve *LAI* from optimal bands of hyper-spectral data; this method can reduce the impact of the canopy non-isotropic features and soil background. To evaluate the performance of the method, Yingke Oasis, Zhangye City, Gansu Province, was chosen as the validation area. This area was covered mainly by maize and wheat. A Hyperion/EO-1 image with the 30 m spatial resolution was acquired on July 15, 2008. Images of 180 m and 1080 m resolutions were generated by linearly interpolating the original Hyperion image to coarser resolutions. Then a multi-scale image serial was obtained. Using the proposed method, we calculated crop area and the average *LAI* of every 1080 m pixel. A SPOT-5 classification figure serves as the validation data of crop area proportion. Results show that the pattern of crop distribution accords with the classification figure. The errors are restrained mainly to −0.1–0.1, and approximate a Normal Distribution. Meanwhile, 85 *LAI* values obtained using LAI-2000 Plant Canopy Analyzer, equipped with GPS, were taken as the ground reference. Results show that the standard deviation of the errors is 0.340. The method proposed in the paper is reliable.

scale transformation, remote sensing, crop yield estimation, simultaneous retrieval, crop area, leaf area index

Remote sensing crop yields estimation is critical for ensuring food security. However, crops are distributed so fragmentally in China that mixed pixels account for a large proportion in moderate and coarse spatial resolution remote sensing images. Therefore, if the crop area is calculated by counting the number of pixels classified as the crop, the accurate estimation is very difficult to implement because of the existence of mixed pixels.

Leaf area index (*LAI*) and crop area are both the key pa-

rameters of remote sensing crop yields estimation. Leaf area index, defined as half the leaf surface area per unit ground surface area [1], can be used to monitor vegetation growth condition [2–5] and estimate crop yield per unit area [6]. If the signal of a mixed pixel is taken as a single one in the retrieval of *LAI*, the retrieved values will deviate significantly from the true values. So, unmixing of mixed pixels becomes a major problem in China to estimate crop yields by means of remote sensing.

Actually, the unmixing of mixed pixels can be expressed approximately by linear matrix equation [7–9]:

*Corresponding author (email: fanwj@pku.edu.cn)

$$X_{I \times J} = A_{I \times N} \cdot \rho_{N \times J}. \tag{1}$$

The matrix X on the left side of eq. (1) is a measurement matrix of $I \times J$ dimensions acquired by sensor, consisting of x value of I mixed pixels and J band series. The matrix A on the right side of eq. (1) describes the area ratio of N components within I mixed pixels; every column vector of matrix A represents the spatial distribution of a certain crop area. Every row vector of matrix ρ describes the spectrum characteristic of each independent component. A variation of some row vector in matrix ρ (spectrum change) mainly reflects the change of *LAI*. Therefore, both matrixes A and ρ are the variables that need to be obtained.

Independent Component Analysis (ICA) can be applied to obtain A and ρ simultaneously, but the preconditions are that: 1) every independent component should satisfy the statistically independent requirement; 2) no more than one independent component's probability density function can be approximated as Gaussian Distribution. However, neither the first nor the second requirement can be satisfied by matrixes A and ρ. The traditional solution is to introduce another independent equation in addition to eq. (1) to make the number of the unknowns balanced with the number of independent equations, which ensures the equation group can be solved. The method proposed in this paper introduces additional information contained in the spatial scaling transformation equation to make the problem solvable, but at the cost of decreasing spatial resolution. This method only provides the crop area and average *LAI* of a coarse resolution pixel, without any information about the crop area and *LAI* for the high resolution pixels direct.

1 The retrieval method

1.1 Canopy BRDF model

Canopy reflectance can be approximated as $\rho = \rho^1 + \rho^m$, where ρ^1 and ρ^m stand for the reflectance contributed by single scattering and multi-scattering respectively [10]:

$$
\begin{aligned}
\rho^1 = \rho_g \Bigg\{ & e^{-\lambda_0 \left[\frac{G_s}{\mu_s} + \frac{G_v}{\mu_v} - \frac{G_v}{\mu_v} \cdot \Gamma(\phi) \right] LAI} \\
& + \left[e^{-\lambda_0 \frac{G_v}{\mu_v} \cdot LAI} - e^{-\lambda_0 \left[\frac{G_s}{\mu_s} + \frac{G_v}{\mu_v} - \frac{G_v}{\mu_v} \cdot \Gamma(\phi) \right] LAI} \right] \frac{E_d}{\mu_s F_0 + E_d} \Bigg\} \\
& + \rho_v \Bigg\{ \left(1 - e^{-\lambda_0 \frac{G_v}{\mu_v} \cdot LAI \cdot \Gamma(\phi)} \right) \\
& + \left[e^{-\lambda_0 \frac{G_v}{\mu_v} \cdot LAI \cdot \Gamma(\phi)} - e^{-\lambda_0 \frac{G_v}{\mu_v} \cdot LAI} \right] \frac{E_d}{\mu_s F_0 + E_d} \Bigg\},
\end{aligned} \tag{2}
$$

where G_V and G_S represent the mean projection of a unit foliage area along the viewing direction and the illuminating direction respectively [11]. $\mu_v = \cos\theta_V$, $\mu_S = \cos\theta_S$, θ_V and θ_S are the viewing zenith angle and solar zenith angle respectively. λ_0 is the Nilson parameter used to describe the clumping effect [12]. $\Gamma(\phi)$ is an empirical function introduced to account for the hot spot effect, where ϕ is the relative angle between viewing and illuminating direction. $\Gamma(\phi) = \exp(-\phi / (\pi - \phi))$, where $0 \leqslant \phi \leqslant \pi$. Therefore, $\Gamma(0) = 1$, $\Gamma(\pi) = 0$. When ϕ varies from 0 to π, $\Gamma(\phi)$ approaches from 1 to 0 in a negative exponential manner. In fact, the empirical function describes the statistical correlation between illuminated and viewed leaves. As for a single leaf, whether an illuminated leaf can be viewed is relevant to the interrelationship between illuminating geometry, viewing geometry and leaf orientation. If leaf orientation is assumed to be isotropic, the correlation between illuminated and viewed leaves depends only on the relative angle between illuminating and viewing orientation for canopy. Thus, using the empirical function, instead of Kuusk model or the like [13, 14], is a balanced approach between accuracy and simplicity. $\mu_S F_0$ is the direct solar irradiance, and E_d is the sky diffuse irradiance. ρ_g and ρ_v are the hemispherical albedos of soil background and leaf respectively. Numerical simulations show that the contribution of multi-scattering can be neglected within 0.68–0.71 and 0.73–0.75 μm, so that single scattering is sufficient to describe the characteristics of canopy bidirectional reflectance [15].

1.2 Removal of background influence—DSD of hyper spectral data

Within 0.68–0.71 μm, the second derivative of leaf spectrum is much larger than that of background spectrum (including soil, water, asphalt and concrete), that is $\rho_v'' \gg \rho_g''$ [15]. Let $L_S = \dfrac{E_d}{\mu_0 F_0 + E_d}$, $b = \lambda_0 \dfrac{G_v}{\mu_v}$, $b' = \lambda_0 \dfrac{G_v}{\mu_v} \Gamma(\phi)$, such that
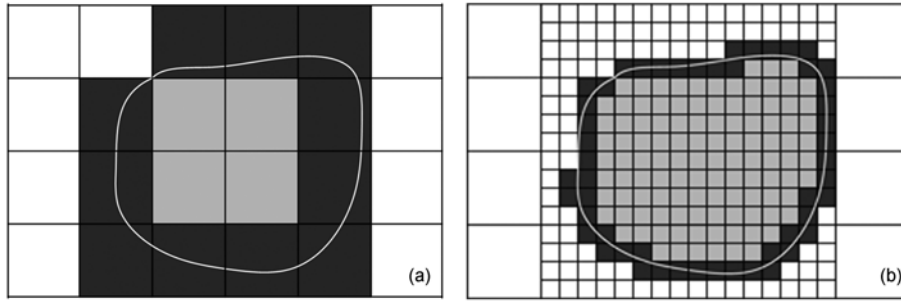
$$x = \frac{\rho''}{\rho_v''} = L_S (1 - e^{-b \cdot LAI}) + (1 - L_S)(1 - e^{-b' \cdot LAI}). \tag{3}$$

Obviously, the DSD method is able to remove background influence effectively, and provides an opportunity to retrieve *LAI* accurately.

1.3 DSD of the mixed pixels

Since the contribution of background spectrum to hyperspectral second derivative can be neglected in certain band, let a_v stand for the area proportion of crop in a mixed pixel, the ratio of the canopy and leaf reflectance spectrum DSDs, x, can be obtained as

Figure 1   A diagram illustrating mixed pixel area of remote sensing images with different resolutions. (a) The coarse resolution case; (b) the high resolution case. The white area is crop, the grey area is heterogeneity, and the black area is mixed pixel.

$$x = \frac{\rho''}{\rho''_v} = a_v[L_s(1 - e^{-b \cdot LAI}) + (1 - L_s)(1 - e^{-b' \cdot LAI})] , \quad (4)$$

where a_v and *LAI* are both unknown variables, so that eq. (4) is uncertain.

1.4   The scale transformation rules

1.4.1   The definition of scale

Suppose the target is composed of crop (which can be approximated as continuous vegetation) and heterogeneity (including all other land use types than crop), which is illustrated in Figure 1. Figure 1(a) and (b) represent remotely sensed images acquired by sensors of different resolutions. It can be seen that mixed pixels always exist on the edge between different land use types. With the increase of spatial resolution, the area proportion of mixed pixels rapidly decreases. Therefore, when the scale decreases to a certain value, the proportion of mixed pixels can be neglected, at which time the area covered by pure vegetation can be considered approximately as the crop area.

Spatial scale corresponds to the spatial resolution of remotely sensed image pixel, *r*. Define the relative scale r_R as [16]

$$r_R = r / r_0 . \quad (5)$$

Here r_0 is spatial resolution of a zero-order scale pixel. At zero-order scale, mixed pixels account for so low a proportion that they can be neglected. If the ratio between the resolutions of two adjacent scales is a constant, *d*, we have

$$r_R = d^n, \quad \text{or} \quad n = \log_d r_R . \quad (6)$$

Here *n* is the scale order. *n*=0 means $r=r_0$, at which time the pixel can be approximated as a pure pixel and retrieved *LAI* from remote sensing images approaches the true value, LAI_0. When $n \geqslant 1$, there is scaling effect in *LAI* retrieval. We denote the *LAI* value retrieved from an *n*-order scale pixel as LAI_n. The scale transformation is used to describe the relationship between LAI_n and LAI_0.
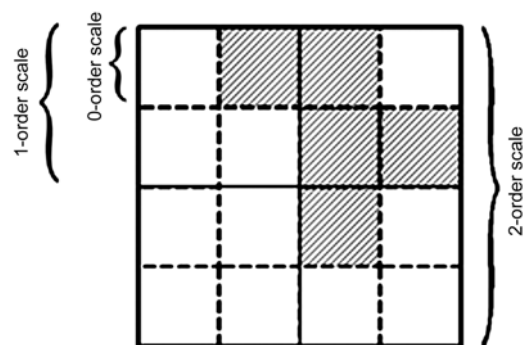
1.4.2   Crop area proportion of different scales

A target can be observed by different sensors with different resolutions, and different results are obtained, which is the so-called "scaling effect" [17, 18]. Suppose a target is observed by 0-order, 1-order, and 2-order scale sensors respectively, as is in Figure 2, in which the shadowed area represents the crop and the white area represents the heterogeneity. A 1-order scale pixel is composed of 2×2 0-order scale pixels and a 2-order scale pixel is composed of 2×2 1-order scale pixels. Let $a_v(n)$ stand for the proportion of crop area in an *n*-order scale pixel, so it is obvious that $a_v(0) \equiv 1$. Thus, the crop area proportion $a_{v,1}$ of the four 1-order scale pixels in Figure 2 is 1/4, 3/4, 0 and 1/4 respectively (first from left to right and then from top to bottom). Therefore, the average crop area proportion of the pixels that are covered at least partly by vegetation, $a_{v,1,a}$, is 5/12. As for the 2-order scale pixel, the area proportion of 1-order scale pixels that are covered at least partly by vegetation, $a_{v,2}$, is 3/4. As a result, for the 2-order scale pixel, $a_v(2) = a_{v,2}a_{v,1,a} = 5/16$, which is the proportion of the crop area in the pixel.

Analogically, $a_v(n) = a_{v,n}a_{v,n-1,a} \cdots a_{v,1,a}$.   Actually, the relationship between $a_v(n)$ and *n* depends on the heterogeneity structure of the target. Since the maximum size of the heterogeneity is finite, the chance that an (*N*+1)-order scale pixel is a pure pixel approaches zero, i.e., $a_{v,N+1} \to 1$, when the size of an *N*-order scale pixel is larger than that of the heterogeneity.

According to numerical simulations, the average $a_v(n)$

Figure 2   An imagined 2-order scale pixel. The shadowed and the white area represent crop and heterogeneity respectively.

satisfies the exponential decline rule [16]:

$$\overline{a_v(n)} = e^{-pn}(1-c) + c. \tag{7}$$

Here c and p are two constants used to describe heterogeneity distribution structure [19]. When $n=0$, $\overline{a_v(0)} \equiv 1$; when $n \to \infty$, $\overline{a_v(n)} \to c$.

1.5 Retrieve $a_v(n)$ and $LAI_{0,a}$ simultaneously using multi-scale data

Suppose a target is observed by sensors of three spatial resolutions, which correspond to 1-order, 2-order, and 3-order scales respectively, and the average second derivatives of the three scales are x_1–x_3 respectively. For an n-order scale pixel, since

$$\rho_n = a_v(n)\rho_0 + [1 - a_v(n)]\rho_g,$$

where ρ_0 represents the reflectance value of a 0-order scale vegetated pixel, which can be expressed by eq. (2). It follows

$$\frac{\rho_n''}{\rho_v''} = a_v(n)\frac{\rho_0''}{\rho_v''}.$$

Therefore, the three average second derivatives of the three scales can be written as the statistical average of the corresponding values of 0-order scale pixels consisted in the larger order scale pixels.

$$x_n = \overline{\frac{\rho_{n,i}''}{\rho_v''}} = \overline{a_{v,i}(n)\frac{\rho_{0,j}''}{\rho_v''}}$$
$$= \overline{a_{v,i}(n)\left[L_s(1 - e^{-b \cdot LAI_{0,j}}) + (1-L_s)(1 - e^{-b' \cdot LAI_{0,j}})\right]}. \tag{8}$$

Here the subscript "0" stands for the 0-order scale, "i" and "j" stand for the ith n-order scale pixel and the jth 0-order scale pixel respectively. Since $a_{v,i}(n)$ and $LAI_{0,j}$ are statistically independent,

$$x_n = \overline{\frac{\rho_{n,i}''}{\rho_v''}} = \overline{a_{v,i}(n)}\cdot\overline{\left[L_s(1 - e^{-b \cdot LAI_{0,j}}) + (1-L_s)(1 - e^{-b' \cdot LAI_{0,j}})\right]}. \tag{9}$$

In consideration of the spatial variation of 0-order scale LAI (LAI_0), let $LAI_{0,j} = LAI_{0,a} + \Delta LAI_{0,j}$ for the jth 0-order scale pixel, where $LAI_{0,a}$ means the average 0-order scale LAI and $\Delta LAI_{0,j}$ is the fluctuation of the jth 0-order scale LAI value from the average value. Thus, the latter part in eq. (9) can be written as

$$\overline{\left[L_s(1 - e^{-b \cdot LAI_{0,j}}) + (1-L_s)(1 - e^{-b' \cdot LAI_{0,j}})\right]}$$
$$= \left[L_s(1 - \overline{e^{-b \cdot (LAI_{0,a} + \Delta LAI_{0,j})}}) + (1-L_s)(1 - \overline{e^{-b' \cdot (LAI_{0,a} + \Delta LAI_{0,j})}})\right].$$

Assuming $\Delta LAI_{0,j}$ obeys Normal Distribution, expand the above term according to Taylor Expansion, in which

$$\overline{e^{-b(LAI_{0,a} + \Delta LAI_{0,j})}} = e^{-bLAI_{0,a}}\overline{e^{-b\Delta LAI_{0,j}}} = e^{-bLAI_{0,a}}\left(1 + \frac{b^2}{2}V_{LAI,0}\right).$$

Here $V_{LAI,0}$ is the variance of the 0-order scale LAI. In order to keep the form of the equation unchanged, an equivalent average 0-order scale LAI, $LAI_{0,a,d}$, is introduced as follow:

$$e^{-bLAI_{0,a,d}} = e^{-bLAI_{0,a}}\left(1 + \frac{b^2}{2}V_{LAI,0}\right).$$

So,

$$LAI_{0,a,d} = LAI_{0,a} - \frac{1}{b}\ln\left(1 + \frac{b^2}{2}V_{LAI,0}\right). \tag{10}$$

According to numerical simulations [16], variance of n-order scale LAI can be approximated as

$$V_{LAI,n} = V_{LAI,0}\cdot e^{-n}, \tag{11}$$

$V_{LAI,n}$ can be obtained from n-order scale remote sensing image, so $V_{LAI,0}$ can be calculated using eq. (11). Therefore,

$$x_n = \overline{\frac{\rho_{n,i}''}{\rho_v''}}$$
$$= \overline{a_{v,i}(n)}\left[L_s(1 - e^{-b \cdot LAI_{0,a,d}}) + (1-L_s)(1 - e^{-b' \cdot LAI_{0,a,d}})\right]. \tag{12}$$

Eq. (12) suggests that the form of the retrieval formula will be the same after introducing an equivalent average 0-order scale LAI, $LAI_{0,a,d}$, if the variation of 0-order scale LAI is taken into account.

Eqs. (7), (10)–(12) can be used to retrieve crop area and the average LAI simultaneously. There are five unknown parameters in the equation group, namely, $LAI_{0,a}$, c, p, b, and b', more than the number of equations, so a remote sensing data series including three scales is needed to solve the problem. Thus, we can get the equation group according to eq. (10)

$$\begin{cases} x_3 = \overline{a_{v,i}(3)}\left[L_s(1 - e^{-b \cdot LAI_{0,a,d}}) + (1-L_s)(1 - e^{-b' \cdot LAI_{0,a,d}})\right], \\ x_2 = \overline{a_{v,i}(2)}\left[L_s(1 - e^{-b \cdot LAI_{0,a,d}}) + (1-L_s)(1 - e^{-b' \cdot LAI_{0,a,d}})\right], \\ x_1 = \overline{a_{v,i}(1)}\left[L_s(1 - e^{-b \cdot LAI_{0,a,d}}) + (1-L_s)(1 - e^{-b' \cdot LAI_{0,a,d}})\right]. \end{cases} \tag{13}$$

At the same time, according to eq. (6),

$$\begin{cases} \overline{a_{v,i}(3)} = e^{-3p}(1-c) + c, \\ \overline{a_{v,i}(2)} = e^{-2p}(1-c) + c, \\ \overline{a_{v,i}(1)} = e^{-p}(1-c) + c. \end{cases} \tag{14}$$

Therefore,

$$\frac{x_3 - x_1}{x_2 - x_1} = \frac{\overline{a_{v,i}(3)} - \overline{a_{v,i}(1)}}{\overline{a_{v,i}(2)} - \overline{a_{v,i}(1)}} = \frac{e^{-2p} - 1}{e^{-p} - 1}. \quad (15)$$

Eq. (15) is a unary quadratic equation, so the unknown parameter p can be obtained by solving the equation and the parameter c can also be calculated easily, which helps to get the a_v value for every coarse resolution pixel. Substituting $\overline{a_{v,i}(n)}$ in eq. (13) for the obtained value, we get

$$x_3 / \overline{a_{v,i}(3)} = L_s(1 - e^{-b \cdot LAI_{0,a,d}}) + (1 - L_s)(1 - e^{-b' \cdot LAI_{0,a,d}}). \quad (16)$$

Substituting $LAI_{0,a,d}$ and x_3 in eq. (16) for the expressions in eq. (10) and (11), $LAI_{0,a}$ can be obtained. In fact, ϕ value of every 0-order scale pixel is not the same with each other. However, in consideration of the narrow sweeping width of 7.5 km for Hyperion/EO-1, ϕ changes only slightly, so the scaling effect of b and b' is neglected in this paper. In order to improve retrieval accuracy, suitable scale series should be designed to decrease the correlation between the three equations.

2 Validations

2.1 Data and pre-processing

The study area is located at Yingke Oaisis, Zhangye City, Gansu Province, 38.75°–39.12°N, 100.33–100.52°E. The Hyperion data used in the work was acquired on July 15, 2008. At that time of the year, the main crops in the region are wheat and maize and the wheat canopy has closed, so it can be approximated as continuous vegetation. This experiment is one part of the "Watershed Allied Telemetry Experiment Research (WATER)" remote sensing experiment [20]. Hyperion image is chosen to retrieve crop area and average *LAI* simultaneously. Onboard EO-1 satellite, Hyperion is a "push boom" instrument with the spatial resolution of 30 m [21]. A Hyperion image covers an area of 180 km×7.5 km [21].
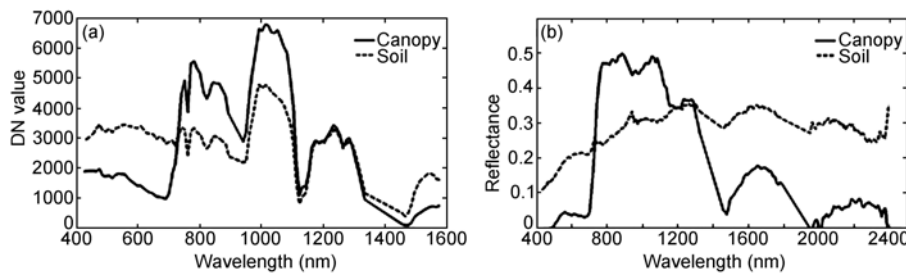
The Hyperion image used in the paper is level L1R, which means that it has been radiometrically corrected, but

not geometrically corrected. Before using Hyperion data quantitatively, a series of pre-processing has to be operated. After geometric correction, those bands that are not calibrated and influenced significantly by moisture among the 242 were deleted, and 47 bands are left in the VNIR spectral range. The image was then transformed to brightness image by radiometric calibration. The strips on the image and SMILE effect were removed using "Global Equilibrium" method [22]. FLAASH (Fast Line-of-sight Atmospheric Analysis of Spectral Hyperion) model was utilized to recover the surface reflectance. Figure 3 is the contrast between the vegetation and soil spectra before and after atmospheric correction, and it indicates that the effect of atmospheric correction is significant. Since the second derivative of spectrum is very sensitive to noises, MNF transformation was conducted to remove some small fluctuations on the spectra, combined with FFT transformation and low pass filter to remove the high frequency part of the spectra.

A multi-spectral SPOT-5 image (the spatial resolution is 10 m) acquired on August 10, 2008 of the same region is used as the validation data. After pre-preprocessing the SPOT-5 image, according to a comprehensive ground investigation, the image was classified into 12 land use types, namely, city, water, wheat, maize, coniferous forest, shrub, street tree, grass, other crops, bare mountain, and sand. The classification accuracy is acceptable. In order to geometrically register SPOT-5 and Hyperion images, geometrically correct SPOT-5 image to Hyperion image, with the accuracy no larger than 0.5 pixel.

2.2 Crop area and average *LAI* retrieval

In order to evaluate the performance of the method, and avoid other error sources such as atmospheric conditions, sun-object-sensor geometry, different band setting, geometric registration and so on, it is determined to use the averaged reflectance value of the 6×6 (the corresponding scale order is 2) and 36×36 (the corresponding scale order is 3) pixels to generate the remote sensing images of the other two scales. The spatial resolutions of 1-order, 2-order, and 3-order images are 30, 180, and 1080 m respectively. Crop area and average *LAI* were retrieved by solving the equation

Figure 3   Contrast of spectra before and after atmospheric correction. (a) DN value before atmospheric correction; (b) reflectance value after atmospheric correction.

groups (13) and (14). The acquisition of the parameter values used in the retrieval is listed in Table 1.
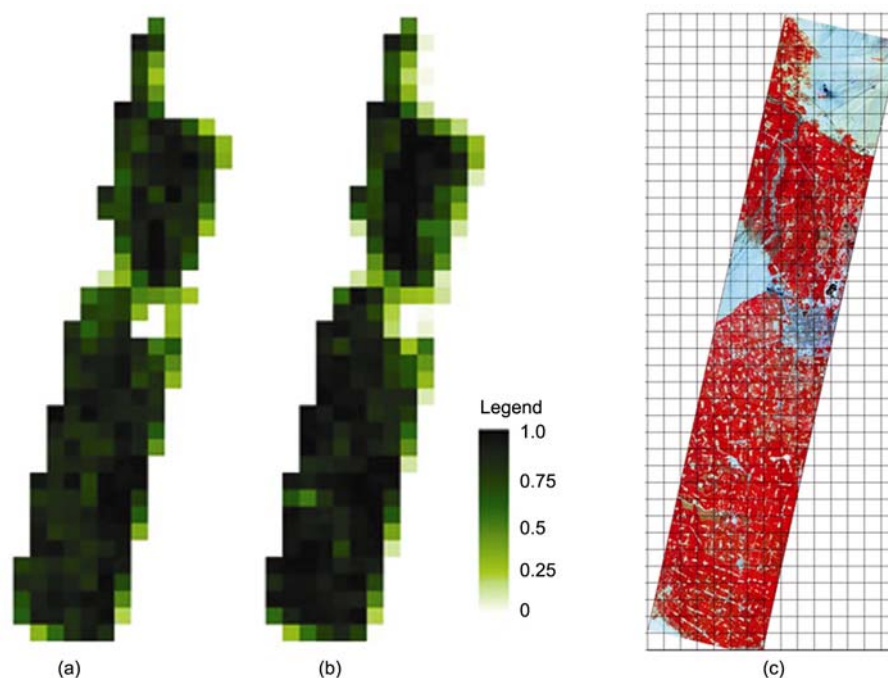
Table 1 Input parameters

Parameter	Meaning	Acquiring method
G function	Foliage angle distribution	Ground measured
θ_v, θ_s	View and solar zenith angles	Acquired from the head file of the remote sensing image
λ_0	Nilson parameter	Average of the results of lower scales
ϕ	Relative angle	Average of the results of lower scales
L_S	The ratio of sky diffuse light	Measured using CE318
ρ_v	Leaf spectrum	Measured using ASD (350–2500 nm)

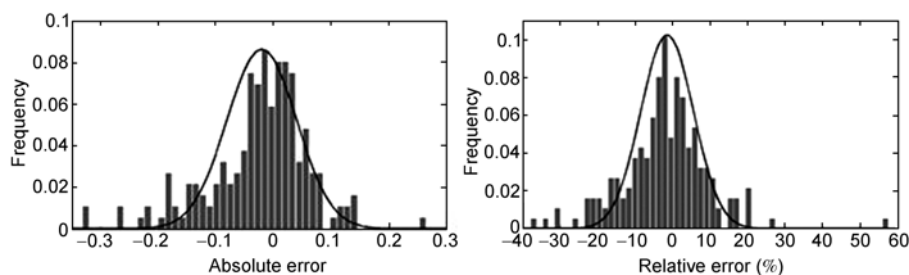## 2.3 Results and error analysis

Figure 4 is a contrast between crop area proportion map obtained using the method given in the paper (a), and one obtained from SPOT-5 classification result (b), and the Hyperion image (c) is also provided as a reference to show the composition of every 3-order scale pixel. It shows that retrieved result agrees well with the validating value as well as with the actual situation.
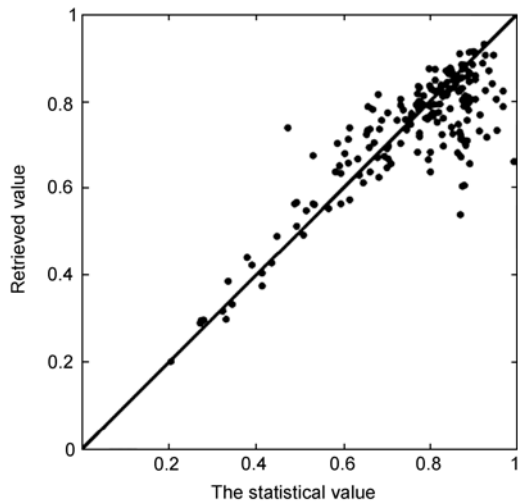
Statistical result from SPOT-5 classification data is taken as the validating data for the retrieved crop area proportion. Histogram analysis is conducted to study the distribution of the retrieval errors (Figure 5). It shows that the retrieval errors obey an approximate Normal Distribution, with the average of −0.026, and the errors mainly distributed within the scope [−0.1, 0.1], with a few values larger than 0.2. The relative errors are also proven to obey Normal Distribution approximately, with an average of −2.127%, and the values mainly fall into the scope [−10%, 10%] (Table 2). It is shown from the scatter points of retrieved values and true values in Figure 6 that the two correlate highly with each other, and the scatter points are distributed near the 45° line.

Figure 4 Retrieved result of crop area proportion. (a) Retrieved result; (b) statistical result from SPOT-5 classification image; (c) hyperion image.

Figure 5 Error distribution of retrieved crop area proportion. The solid line represents the normal distribution plot.
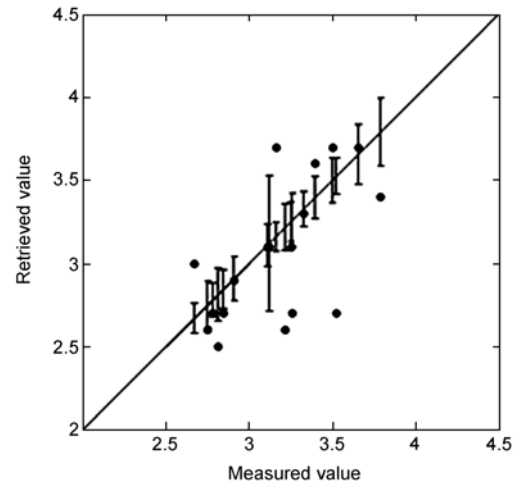
Figure 6 Validation of the retrieved crop area propotion. The statistical value is the value obtained from SPOT-5 classification result, and the retrieved value is the one calculated using the method of the paper.

Table 2 Error analysis of retrieved crop area proportion

	Average	Standard deviation	Minimum error	Maximum error
Absolute error	−0.026	0.086	2.630×10^{-4}	0.331
Relative error (%)	−2.127	11.414	0.030	56.104

The *LAI* values measured by LAI-2000 Plant Canopy Analyzer, equipped with GPS, on July 14 and 15, 2008 around 50 km^2 area scope in Yingke Oasis are used as the validating dataset for retrieved average *LAI*. There are 85 measurements in the area covered by the image, and they distribute in 21 3-order scale pixels, whose spatial resolution is 1080 m. Among the 21 3-order scale pixels, 3 are complex because of the large growing condition difference, while only 1 measurement is taken in the ground experiment, which is not enough to show the real condition of the 3-order scale pixel. So, only 18 3-order scale pixels are applied to validate the accuracy. First, the measured values in every 3-order scale pixel are averaged as the true average *LAI* of the pixel to validate the retrieved result. Figure 7 is a contrast between the true and retrieved values. Table 3 shows that the average error is −0.11, with the minimum and maximum values of 0.01 and 0.825 respectively. The average relative error is −3.28%, with large values for a few pixels. Figure 7 shows that the retrieved values are generally smaller than the measured ones, due to the existence of scale effect in the validation process. The corresponding spatial resolution of a 0-order scale pixel is 5 m, at which size pure pixels account for a very large percentage, but mixed pixels also exist, which indicates that there is still heterogeneity in the 0-order scale pixels.

Figure 7 Scatter of measured *LAI* and retrieved *LAI*. The erect lines in the figure illustrate the range of *LAI*±std measured by LAI-2000 Plant Canopy Analyzer.

Table 3 Error analysis of retrieved average *LAI*

	Average	Standard deviation	Minimum error	Maximum error
Absolute error	−0.110	0.340	0.010	0.825
Relative error (%)	−3.279	10.427	0.322	23.404

3 Conclusions and discussion

In consideration of highly fragmented crops and general existence of mixed pixels in china, this work develops a method to retrieve average *LAI* and crop area simultaneously and accurately for mixed pixels from coarse resolution remote sensing images with the aid of multi-scale remote sensing data series. In a rigorous way, this method does not belong to unmixing of mixed pixels, but it is just a traditional approach, providing an opportunity to retrieve the two parameters at the same time based on the information given by scale transformation rules at the cost of spatial resolution decrease.

Conceptually, the proportion of crop area in an individual mixed pixel is unpredictably random. In order to implement information separation for mixed pixels, we have to turn to statistical methods for help. In fact, either Independent Component Analysis (ICA) or the method in the paper belongs to statistical method, which explains why it is at the cost of spatial resolution decrease. For statistics, the values of individual samples may deviate from the average value significantly. However, practices show that the annual variations of crop area and crop yields are smaller than 5%. Therefore, if this method is applied to monitor crop growth condition by means of remote sensing, the key is how to improve monitoring accuracy. Obviously, the difficulty does not lie in improving measure accuracy, lowering calculation errors or the like, but in the fact that statistical

method is not good at predicting small probability events. In a word, it requires further work before crop yield estimation can be implemented in China.

1   Chen J M, Black T A. Defining leaf area index for non-flat leaves. Plant Cell Environ, 1992, 15: 421–429
2   Badhwar G D, MacDonald R B, Metha N C. Satellite-derived leaf-area-index and vegetation maps as input to global carbon cycle models—A hierarchical approach. Int J Remote Sens, 1986, 7: 265–281
3   Baret F, Guyot G. Potentials and limits of vegetation indices for LAI and APAR assessment. Remote Sens Environ, 1991, 35: 161–173
4   Bonan G B. Land-atmosphere interactions for climate system models: Coupling biophysical, biogeochemical, and ecosystem dynamical processes. Remote Sens Environ, 1995, 51: 57–73
5   Bicheron P, Leroy M. A method of biophysical parameter retrieval at global scale by inversion of a vegetation reflectance model. Remote Sens Environ, 1999, 67: 251–266
6   Mass S J. Use satellite data to improve model estimates of crop yield. Agron J, 1988, 80: 655–662
7   Xu X R, Zhou L F, Zhu X H. Factor-analysis method of mixed pixel and its application to estimation of winter-wheat in large area. Chin Sci Bull, 1989, 35: 317–320
8   Fan W J, Xu X R. A method for blind separation of components information from mixed pixel. Prog Nat Sci, 2006, 16: 760–765
9   Tao X, Fan W J. Blind separation of component information from hyperspectral data. Acta Sci Nat Univ Pekinensis, 2008, 1: 73–78
10   Jin H R, Tao X, Fan W J, et al. Monitor the spatial distribution of leaf area index in the high resolution pixel based on BJ-1 data (in Chinese). Prog Nat Sci, 2007, 17: 1229–1234
11   Ross J. The radiation regime and architecture of plant stands. The Hague-Boston-London: W. Junk Publishers, 1981
12   Nilson T. A theoretical analysis of the frequency of gaps in plant stands. Agric Meteorol, 1971, 8: 25–38
13   Kuusk A. The hot spot effect of a uniform vegetative cover. Sov J Remote Sens, 1985, 3: 645–658
14   Jupp D, Strahler A H. A hotspot model for leaf canopies. Remote Sens Environ, 1991, 38: 193–210
15   Fan W J, Xu X R, Liu X C, et al. The accurate LAI retrieval method based on PROBA/ CHRIS data. Hydrol Earth Syst Sci, 2010, in press
16   Xu X R, Fan W J, Tao X. The spatial scaling effect of continuous canopy Leaves Area Index retrieved by remote sensing. Sci China Ser D-Earth Sci, 2009, 52: 393–401
17   Chen J M, Black T A. Measuring leaf area index of plant canopy with branch architecture. Agric Meteorol, 1991, 57: 1–12
18   Chen J M. Spatial scaling of a remotely sensed surface parameter by contexture. Remote Sens Environ, 1999, 69: 30–42
19   Tao X, Yan B Y, Wang K, et al. Scale transformation of leaf area index product retrieved from multi-resolution remotely sensed data analysis and case studies. Int J Remote Sens, 2009, 20: 5383–5395
20   Li X, Ma M G, Wang J, et al. Simultaneous remote sensing and ground-based experiment in Heihe River Basin: Scientific objectives and experiment design. Adv Earth Sci, 2008, 23: 897–914
21   Beck R. EO-1 User Guide Version. 2.3. http://eo1.usgs.gov, 2003
22   Tan B X, Li Z Y, Chen E X, et al. Processing of EO_1Hyperion hyperspectral data (in Chinese). Remote Sens Inf, 2005, (6): 36–47